Plasma Sources Sci. Technol. **5** (1996) 193–199. Printed in the UK

Study of plasma–surface interactions: chemical dry etching and high-density plasma etching

G S Oehrlein, P J Matsuo, M F Doemling, N R Rueger, B E E Kastenmeier, M Schaepkens, Th Standaert and J J Beulens

Department of Physics, State University of New York, Albany, 1400 Washington Avenue, Albany, NY 12222, USA

Received 8 November 1995, in final form 4 January 1996

Abstract. We report results of the characterization of the plasma–surface interactions of silicon and silicon dioxide in fluorocarbon discharges using real-time ellipsometry and post-plasma multi-technique surface analysis for chemical dry etching (CDE) and high-density plasma etching (HDPE). We show that changes of the gas composition in CDE causes major changes in silicon surface chemistry and etching behaviour. For low-pressure HDPE we investigate the influence of power deposition into the discharge and bias voltage and bias power at the wafer on the surface chemical changes of silicon and SiO_2.

1. Introduction

The rate of an etching reaction in a low-pressure plasma can often be directly related to the thickness and composition of the surface reaction layer formed on the film that needs to be etched in this environment [1, 2]. In turn, the characteristics of the surface reaction layer are primarily controlled by the chemical composition of the discharge, the ion bombardment energy and ion fluxes at the substrate [3]. Most published work has been performed using capacitatively coupled RF powered reactors. In this article we report results obtained using chemical downstream etching (CDE) and high-density plasma etching (HDPE). Both CDE and HDPE are based on remote plasma sources and are designed to control plasma–surface interactions to a much greater extent than is possible in plasma processing using traditional capacitatively coupled devices. In CDE the charge density decays along the transport tube and no bias is applied to the wafer [4–6]. The density of ions at the wafer surface is negligible and the surface chemical changes are dominated by reactive neutral radicals and metastable species. In low-pressure HDPE the ion/neutral ratio is high, and the plasma–surface interactions are controlled by the impact of energetic ions. The ion density is controlled by the input power to the plasma source. Separate RF biasing is used to control the energy of the ions that strike the substrate.

In the first part of this paper we show that the surface modifications of silicon in CDE are unexpected. Very thick reaction layers can form (of the order 10 nm), and small changes of the input gas mixtures can change in a significant way the silicon etching behaviour and its surface modifications. We also show that the substrate surface can change significantly after the discharge has been extinguished. In the second part of the paper we examine the question of whether ion energy or ion power is the key variable that determines the disorder in a Si substrate exposed to a low-pressure high-density plasma with independent RF bias. We show that for a situation where significant steady state etching occurs, ion power is the more important variable, whereas for highly selective etching (very low etch rate) ion energy is the variable that determines residual damage. The effect of these parameters on the steady state fluorocarbon film formed on the silicon surface that is responsible for the achievement of SiO_2/Si etch selectivity is also reported. Fluorocarbon films also form on SiO_2 surfaces for low ion bombardment energies and limit the SiO_2 etch rate. The relationship between fluorocarbon film thickness in SiO_2, its stoichiometry and RF voltage is discussed in the last part of the paper.

2. Experiment

The experiments were performed in a multi-chamber apparatus capable of handling 125 mm wafers. The CDE and HDPE process chambers are connected via a central wafer handler to a multi-technique surface analysis system for post-plasma surface analysis and a load-lock chamber for sample introduction. The mounting of the samples on an electrostatic chuck which is cooled to a temperature of 10 °C is the same in both chambers. A pressure of 5 Torr of helium is applied to the rear of the wafer. The

0963-0252/96/020193+07$19.50

diagnostics, e.g. ellipsometry, mass spectrometry, optical emission spectroscopy, etc, are also the same. Details on the two process chambers follow.

The ultrahigh vacuum-compatible microwave-based CDE apparatus has been described previously [7]. Briefly, a microwave plasma is produced in an ASTeX DPA-38 microwave plasma applicator. This device is equipped with a 38 mm od, 1.5 mm thick quartz tube to which the process gases are fed. The microwave power (2.54 GHz) was kept constant at 400 W for this work. The sample is located in a cylindrical process chamber (inner diameter 27 cm, height 30 cm) with water-cooled walls. The system is pumped using a turbomolecular pump backed by a roots blower and a vane pump. For the experiments described here, the pressure was kept at 500 mTorr. A throttle valve was used to control the pumping speed and maintain this pressure in the chamber. If the microwave applicator is connected directly to the dry etching chamber, the species produced in the microwave discharge have to travel horizontally a distance of 30 cm to reach the sample ('zero tube length'). We also examined the effect of inserting transport tubes of various lengths (up to 125 cm) made of either quartz or Teflon between the microwave discharge and the reaction chamber, but will not report those results here. Gas mixtures of $CF_4/O_2/N_2$ were examined. The flow of CF_4 was fixed at 400 sccm and the ratio of O_2/CF_4 or N_2/CF_4 was varied and will be reported.

The inductively coupled plasma (ICP) tool used in this work has previously been described by Bell *et al* [8] and is similar to the apparatus reported by Keller *et al* [9]. A planar induction coil, supplied with 0–2000 W RF power at 13.56 MHz, generates the plasma through a 16 mm thick quartz window. The distance between wafer and induction coil is 7 cm. For the present experiments we used CF_4 and CHF_3 plasmas generated with 1400 W inductive power in the pressure range of 6 to 20 mTorr at a constant gas flow of 40 sccm. Different amounts of 3.4 MHz bias power were applied to the electrostatic chuck to change the self-bias voltage over the range 0 to -200 V. The self-bias voltage was measured by making direct contact to the wafer.

The samples consisted of thin films of SiO_2, Si_3N_4 polycrystalline silicon on a 100 nm layer of SiO_2 on Si (100) or just Si (100) wafers.

3. Downstream etching of silicon

Figure 1 shows the etch rate of poly-Si in $CF_4/O_2/N_2$ as a function of added O_2 and N_2 using 400 W microwave power, 500 mTorr pressure and a constant flow of 400 sccm CF_4. For CF_4/O_2 mixtures without N_2 we see the well known increase of the etch rate as small amounts of oxygen are injected, due to the increase of F atom concentration by oxidation of CF_x radicals [10–12]. At high percentages of O_2 the etch rate decreases due to surface oxidation of silicon [2]. Upon injection of 5% N_2 (20 sccm) the poly-Si etch rate increased by an additional factor of two relative to values without N_2 at the etch rate maximum. Adding 10 or 15% of N_2 resulted in no further increase of the poly-Si etch rate at the etch rate maximum. For oxygen-rich gas mixtures a more rapid decrease of the etch rate

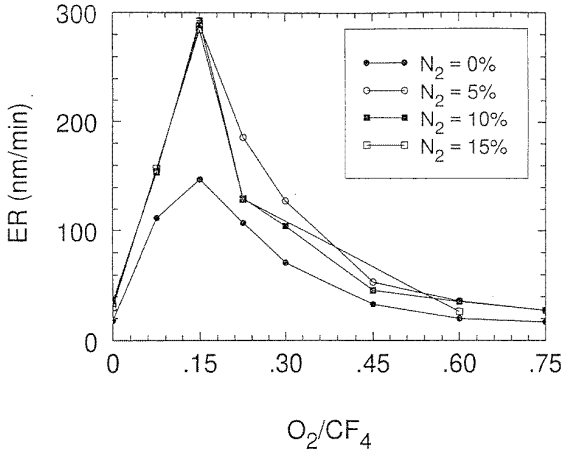

Figure 1. The dependence of the poly-silicon etch rate on O_2/CF_4 ratio without N_2 and with 20, 40 or 60 sccm N_2. Conditions: 500 mTorr, 400 W, CF_4 flow = 400 sccm.

at high O_2/CF_4 ratios is seen, however, and is indicative of enhanced oxidation. Just adding N_2 to CF_4 without O_2 does not result in a significant enhancement of the Si etch rate. Therefore, both O_2 and N_2 must be added to CF_4 to maximize the etch rate. In addition, both have to be injected into the discharge region.

Even more significant enhancements of the Si_3N_4 etch rate were observed upon injection of 5% N_2 (by a factor 7× for a O_2/CF_4 ratio of 0.15) [13], but are not reported here for brevity. Careful examination of the fluorine density in the discharge region and in the downstream chamber showed that N_2 injection did not increase the F atom concentration. A survey of all mass peaks resulted in the conclusion that NO is the important species that is formed if O_2 and N_2 are both injected into the discharge region. The Si_3N_4 etch rate correlates directly to the NO mass spectrometric signal. Since for Si_3N_4 the breaking of the SiN bond is one of the key steps in the overall etching reaction, the role of NO was postulated to be in the removal of N from the Si_3N_4 surface by direct reaction with N to form N_2 or possibly N_2O. The role of NO in the enhancement of the Si etch rate is less clear and has been discussed by Matsuo *et al* [14]. In the following we will show that etch rate changes in silicon are accompanied by dramatic changes in the surface reaction layer.

Figure 2 shows real-time ellipsometry data obtained during microwave induced chemical dry etching of single-crystal silicon. The silicon surface had been cleaned using hydrofluoric acid prior to the experiment. A high proportion of O_2 in CF_4 was used for this experiment ($O_2/CF_4 = 0.75$) and initially no N_2 was present. The ellipsometric angles delta and psi are plotted. At point (a) the CF_4/O_2 microwave discharge is ignited. The decrease of delta and increase of psi can be interpreted by the growth of a transparent layer on the silicon surface. We observe the rapid formation of a SiO_xF_y reaction layer to a saturation thickness which is reached within several seconds. The thickness then no longer changes, and steady state etching of the silicon takes place at a rate given in figure 1. At time (b) we inject additionally 5% of N_2 into the O_2/CF_4

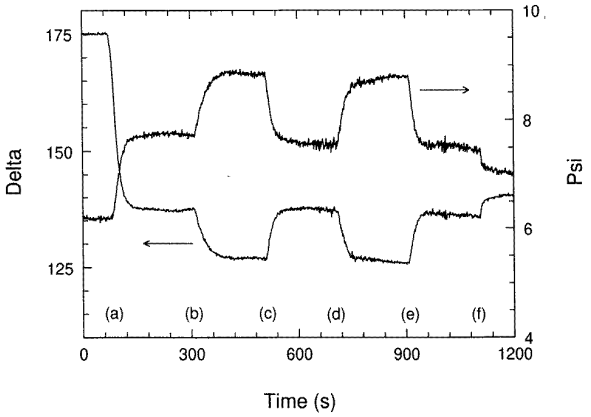

Figure 2. Real-time ellipsometry data before, during and after microwave induced CDE of single-crystal silicon using O_2/CF_4 = 0.75. At (*a*) the microwave discharge is ignited. The formation of a reaction layer on the unperturbed silicon occurs ($\approx$ 10 nm thick). At (*b*) 20 sccm N_2 is injected in addition and leads to an increase of the thickness of the reaction layer (to $\approx$ 11 nm). At (*c*) the N_2 flow is stopped. The thickness of the reaction layer decreases again. At (*d*) N_2 is injected again and the reaction layer thickness increases again. At (*e*) the N_2 supply is shut off once more and at (*f*) the microwave plasma is extinguished and the chamber is evacuated.

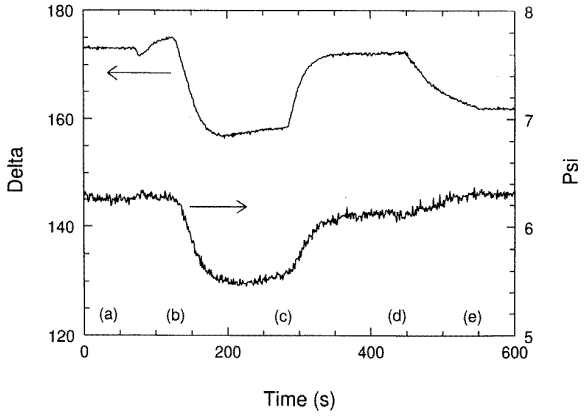

Figure 3. Real-time ellipsometry data for chemical dry etching of single-crystal silicon using O_2/CF_4 = 0.15. At time (*a*) the discharge is ignited and tuned. Tuning is complete at (*b*), and a thin reaction layer grows. This layer may be interpreted as being due to surface roughness. At time (*c*) 20 sccm N_2 is injected. At time (*d*) the discharge is terminated. At time (*e*) it is evacuated.

mixture. From figure 1 we know that this results in an increase of the etch rate. Surprisingly, the thickness of the reaction layer increases upon N_2 injection. These changes are highly reproducible, as shown by the other experiments of figure 2. The thicknesses of the reaction layers are also surprising: at point (a) a reaction layer of about 10 nm thickness is formed, which then increases to 11 nm at point (b). These thicknesses are nearly by a factor of 10$\times$ greater than those seen in 25 mTorr RIE [2] using CF_4/O_2 and imply complex film formation and diffusion processes in CDE of Si when both high levels of fluorine and oxygen are employed.

Silicon surfaces processed using O_2-rich gas mixtures remained smooth during the etching experiments. The formation of the surface reaction layers occurred within a few seconds and then no longer changed. When gas mixtures with little O_2 were used, surface roughness effects were sometimes pronounced, and the surface changed continuously during the etch experiment. The formation of surface roughness is due to the high selectivity between etching Si and SiO_2 and high Si etch rates for the fluorine-rich discharges if only small amounts of O_2 are employed. When the native oxide was carefully removed from the Si surface prior to the CDE experiment, a steady state film was formed. This is shown in figure 3 for a O_2/CF_4 = 0.15 gas mixture. At point (a) the microwave is ignited. Initially tuning is required to minimize reflected power. Subsequently a modified layer forms on the silicon surface. At point (c) 5% N_2 is injected in addition. We then see the removal of the layer which initially had been formed. We also note that in this experiment delta and psi both decrease. This indicates that an absorbing layer (complex refractive index) is formed in this case. The data can be interpreted by the formation of a rough silicon surface. Injection of N_2 leads to the removal of this roughness and the formation of a Si surface with only a very thin reaction layer. We also note that in this case after extinction of the microwave discharge, a transparent surface reaction layer forms (delta decreases, psi increases). The Si surface formed by $CF_4/O_2/N_2$ CDE and/or the decaying plasma is apparently very reactive. The changes that occur to this surface upon plasma extinction dominate the surface modifications, and the results of the post-plasma surface analysis experiments have little relevance to the surface chemistry that dominates the etching.

A comparison of the relative changes of the reaction layer that occur upon extinguishing the discharge are displayed in figure 4 for O_2/CF_4 = 0.15 and O_2/CF_4 = 0.75 gas mixtures with and without 5% N_2 as traces (a), (c), (b) and (d) respectively. For case (a) the reaction layer does not change appreciably. For (b) it grows by 0.93 nm. For the O_2-rich gas compositions thick layers are formed and the reaction layers decrease by up to 2 nm in thickness after extinction of the discharge. It is clear from figure 4 that for CDE applications real-time surface analysis may be essential for interpreting etch rate data and also that the relevance of post-plasma surface analysis data needs to be determined on a case by case basis.

The above data show that CDE related surface processes are complex and can be difficult to study. Whereas for direct plasma etching and deposition processes well defined and dramatic differences between the plasma on state and the plasma off wafer state exist, e.g. in the ion bombardment of the wafer surface, the differences between these states are less dramatic for CDE if the processing takes place far away from the discharge zone. For a direct plasma process the surface state appears to be frozen once the ion bombardment is removed by extinguishing the discharge [3, 15–17]. For CDE, etching reactions can continue for a significant time after the discharge has been extinguished and are just a natural continuation of the

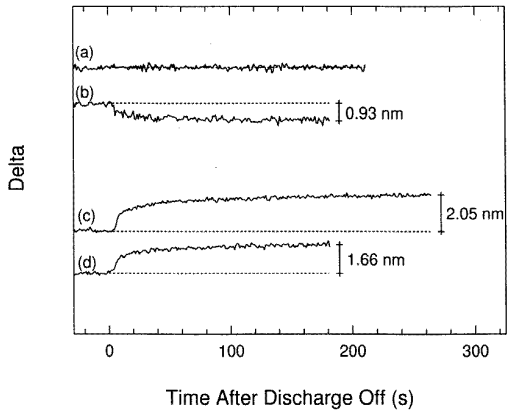

Figure 4. Changes of the reaction layer as a function of time after extinguishing the microwave discharge. The $CF_4/O_2/N_2$ flows were: (*a*) 400/60/0; (*b*) 400/60/20; (*c*) 400/300/0; (*d*) 400/300/20. The change in layer thickness (in nm) from the discharge-on value is also indicated.

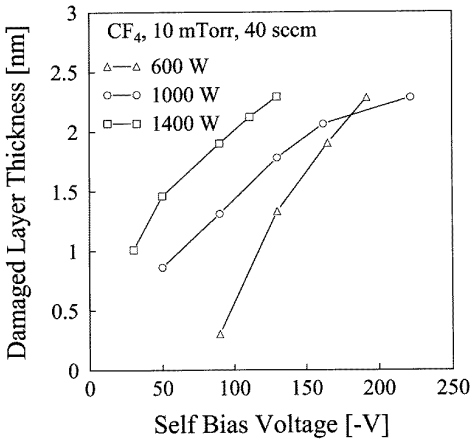

Figure 5. Damaged layer thickness as a function of dc self-bias voltage for a CF_4 ICP high-density plasma. The pressure in the experiment was held constant at 10 mTorr, and the inductive power was varied from 600 W to 1400 W.

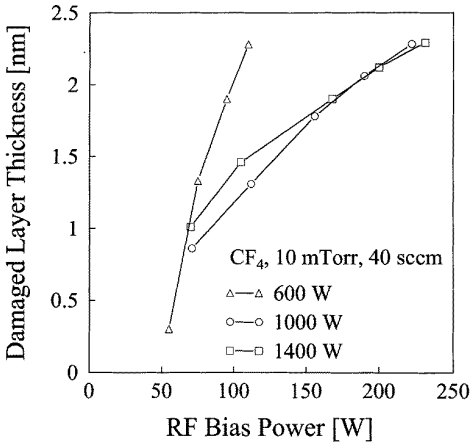

Figure 6. The data of figure 5 plotted versus RF bias power.

CDE process. Real-time surface analysis methods are the technique of choice for the study of these processes.

4. High-density plasma etching of Si and SiO_2

4.1. Silicon

The modifications of a silicon surface exposed to a high-density plasma consist of the formation of a thin fluorocarbon film and of a disordered silicon surface region and these modifications can be simultaneously quantified by an ellipsometric measurement [18]. The fluorocarbon film is required for obtaining SiO_2/Si etch selectivity. The disordered Si surface layer is determined by the ion bombardment of the surface. We examine here the effect of RF bias power and RF bias voltage on the thickness of the Si disordered layer and the thickness of the fluorocarbon film.

In figures 5 and 6 we plot the thickness of the disordered Si layer determined by ellipsometry versus self-bias voltage (figure 5) or RF bias power (figure 6) for a CF_4 discharge. Three different inductive powers were used (600 to 1400 W). For the ICP the ion current to the substrate increases linearly with inductive power at constant pressure and gas flow. The RF bias power required to produce a certain self-bias voltage increases therefore with inductive power. Figures 5 and 6 show that the Si disorder intensity increases with self-bias voltage and RF bias power. Self-bias voltage does not uniquely determine the damaged layer thickness. In general a better correlation between damaged layer thickness and RF bias power is seen for CF_4. For this etching gas the silicon steady state etch rate is fairly high (up to 200 nm min^{-1}). In figure 7 we show the steady state fluorocarbon film thickness as a function of self-bias voltage.

The intensity of damaged silicon is also determined by the fluorocarbon steady state film thickness. For 600 W inductive power we see a rapid decrease with self-bias voltage, whereas for 1000 W and 1400 W inductive power we observe an increase. For the latter samples the intensity of Si disorder is nearly identical for a given self-bias voltage, whereas for the 600 W sample it increases at a much greater rate with RF bias power.

In figures 8 and 9 we show equivalent Si disorder data for CHF_3. For this gas the silicon surface is covered with a much thicker fluorocarbon film (see figure 10), and the Si etch rate is much smaller than for CF_4 ($\sim$ 20 nm min^{-1} at 1400 W inductive power). The steady state thickness of the fluorocarbon film increases strongly with inductive power and is always significantly greater than seen for CF_4. The thickness of the damaged Si layer correlates in this case much better to self-bias voltage than to RF bias power. Consistent with the thicker fluorocarbon film, the thickness of the damaged Si layer is much smaller for a given self-bias voltage than for the CF_4 case.

Figure 10 shows that the steady state fluorocarbon film thickness on Si is primarily determined by inductive power and actually increases with self-bias voltage. We now show that this is opposite to what is seen for SiO_2. This explains why SiO_2/Si etch selectivity can increase with self-bias voltage.

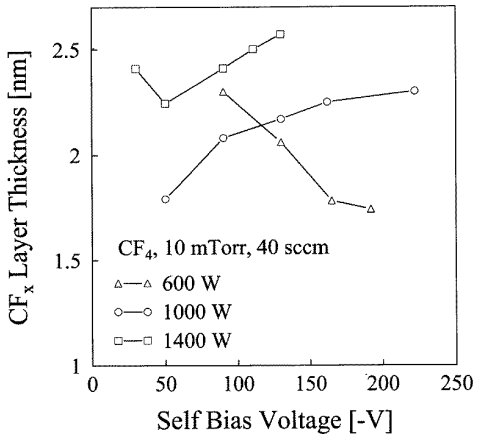

Figure 7. The steady state fluorocarbon film thickness corresponding to the samples of figure 5 as a function of dc self-bias voltage.

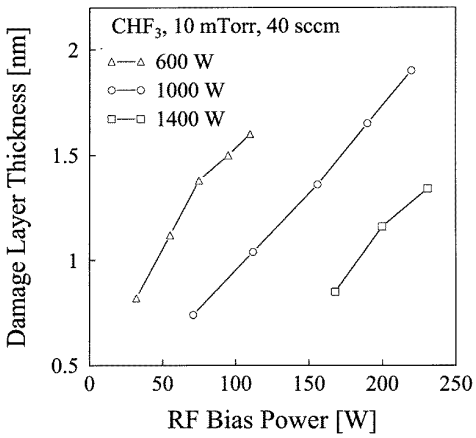

Figure 9. The data of figure 8 plotted versus RF bias power.

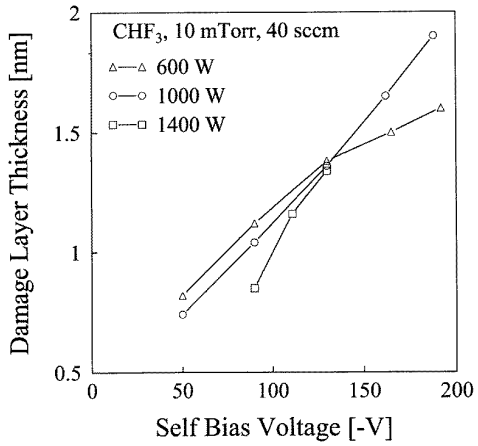

Figure 8. Damaged layer thickness and fluorocarbon film thickness as a function of dc self-bias voltage for a CHF_3 ICP high-density plasma. The pressure in the experiment was held constant at 10 mTorr, and the inductive power was varied from 600 W to 1400 W.

4.2. Silicon dioxide

The SiO_2 etch rate in an electron cyclotron resonance (ECR) fluorocarbon plasma exhibits a *fluorocarbon deposition* regime at low RF bias power, a *fluorocarbon suppression* regime for intermediate RF bias conditions and an *oxide sputtering* regime at high RF bias [19]. Figure 11 shows the SiO_2 etch rate measured in an ICP CHF_3 plasma at 10 mTorr produced using 1000 W inductive power as a function of self-bias voltage. This curve exhibits the same three regimes.

In previous ECR work it has been shown that in the fluorocarbon suppression regime a thin fluorocarbon film covers the SiO_2 surface during steady state etching [20]. The film thickness decreases rapidly with RF bias voltage. In the current ICP studies we have carefully determined the fluorocarbon steady state film thickness and measured the SiO_2 etch rate at the same time. Figure 12 shows the SiO_2 etch rate plotted versus the inverse of the fluorocarbon film thickness. We see that in the fluorocarbon suppression regime the SiO_2 etch rate increases in a roughly linear fashion with inverse steady state film thickness. This behaviour is similar to that seen for Si etching [1], but the SiO_2 etch rate shows a much stronger dependence on the fluorocarbon film thickness. As the fluorocarbon film varies in thickness from 0.63 nm to 0.32 nm (in inverse thickness 1.59 to 3.13 nm^{-1}) the SiO_2 etch rate increases from 114 nm min^{-1} to 481 nm min^{-1}. For slightly thicker fluorocarbon films the etching of SiO_2 stops. The stronger dependence of the SiO_2 etch rate on fluorocarbon film thickness should be related to the overriding importance of ion bombardment [21, 22] and *direct reactive ion etching* for SiO_2; as the steady state fluorocarbon film thickness grows, an increasing fraction of the energy of the ions is dissipated in this film and can no longer break Si–O bonds and etching of the SiO_2 stops. For silicon etching we observe etching for much thicker films, e.g. silicon etches at a rate of $\sim$ 10 nm min^{-1} for a fluorocarbon film thickness of about 6 nm shown in figure 10. This is consistent with the spontaneous reaction rate of fluorine atoms with silicon. This reaction will occur once fluorine has diffused through the fluorocarbon film to the silicon surface. Bombarding the fluorocarbon film and enhancing the diffusion of fluorine atoms to the fluorocarbon film/silicon interface will be sufficient to induce silicon etching, but will not lead to SiO_2 etching.

Figure 13 shows the fluorine/carbon ratio of the fluorocarbon films that is present during steady state etching on the SiO_2 surface as a function of self-bias voltage. We see that as the RF bias voltage is increased, the F/C ratio rapidly decreases and stabilizes at a value of about 0.6. These data may be interpreted by ion induced etching of the SiO_2 and the steady state CF_x layer. We have determined that the average stoichiometry of the particle flux that produces the fluorocarbon film is less than two (from the stoichiometry of the film grown without RF bias). If we postulate SiF_4 and CO as the primary etch products, there will be some excess carbon that will remain on the SiO_2 surface as etching proceeds. As the SiO_2 etch rate increases, the excess carbon left over from the SiO_2 etching reaction becomes more important and the F/C ratio of the remaining fluorocarbon material decreases. Ion induced etching will also dissociate F–C bonds and drive an

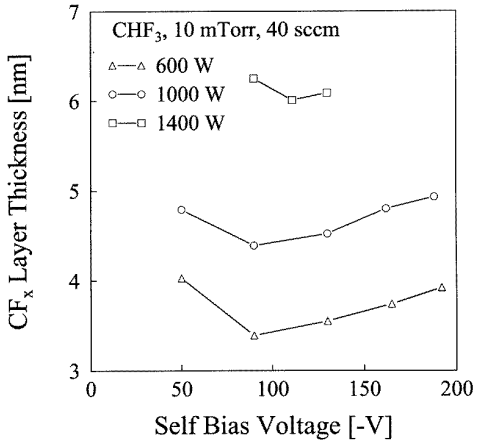

Figure 10. The steady state fluorocarbon film thickness corresponding to the samples of figure 8 as a function of a dc self-bias voltage.

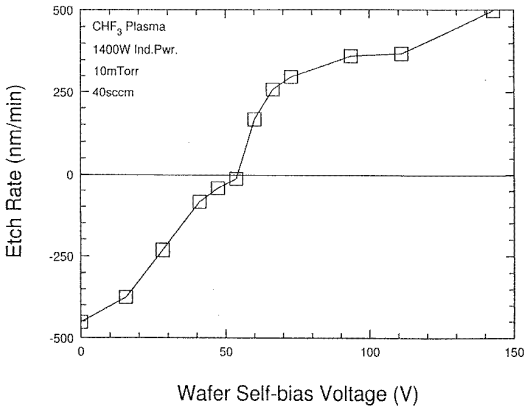

Figure 11. The dependence of the SiO_2 etch rate in a CHF_3 ICP high-density plasma on self-bias voltage. Experimental conditions: 10 mTorr pressure, 1000 W 13.56 MHz inductive power, 40 sccm CHF_3, variable 3.4 MHz RF bias power.

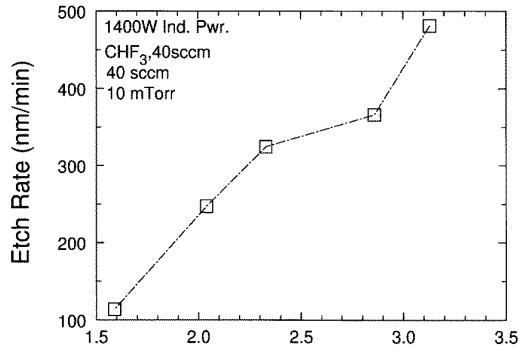

Figure 12. The SiO_2 etch rate versus the inverse of the steady state fluorocarbon film thickness in the fluorocarbon suppression regime.

etching reaction of the fluorocarbon film via CF_4 formation (or other volatile products). This reaction decreases the

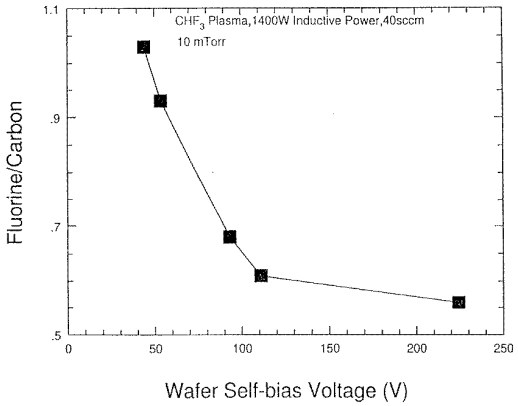

Figure 13. The fluorine/carbon ratio of the fluorocarbon film that exists on the SiO_2 surface versus self-bias voltage.

F/C ratio of the residual fluorocarbon layer. Ultimately the fluorocarbon film is so thin that primarily the stoichiometry of the incoming particle fluxes and the etching of SiO_2 will determine the F/C ratio of the residual film. The F/C ratio then only changes slowly as the SiO_2 etch rate increases as the square root of the ion bombardment energy [20]. For silicon the reduced F/C ratio of the fluorocarbon film at increasing RF bias voltage leads to a slow increase of the steady state film thickness (see figure 10).

5. Conclusions

For CDE, gas composition plays a key role in determining silicon surface processes during etching. Many of the observations are not obvious, e.g. N_2 injection into CF_4/O_2 leads to increased etching, but can result in a thinner or thicker reaction layer, depending on the O_2/CF_4 ratio that is used. The reaction layers can be extremely thick, e.g. in excess of 10 nm. Nitrogen incorporation in the surface after etching is very small. We note that, depending on the state of the surface that is formed during CDE, both reaction layer growth or thinning after extinction of the microwave discharge may take place. This fact greatly complicates the interpretation of post-plasma surface analysis data and shows that real-time surface analysis methods are the techniques required for the study of these processes.

In fluorocarbon high-density plasmas the etching of both Si and SiO_2 can be controlled by a thin steady state fluorocarbon film. This film is responsible for SiO_2/Si etch selectivity, since for SiO_2 the fluorocarbon film thickness rapidly decreases with RF bias voltage, whereas for Si it actually increases with self-bias voltage. For CF_4, RF power rather than RF voltage is the parameter that controls surface disorder. For CHF_3, however, RF voltage is the parameter that controls Si disorder. This difference must be related to the facts that (1) the fluorocarbon film thickness is much smaller for CF_4 than for CHF_3, allowing a greater proportion of all ions to contribute to introduction of Si disorder; and (2) that significant steady state etching of the silicon substrate occurs for CF_4.

Acknowledgments

This work was supported by SEMATECH, Sandia National Laboratories and the New York State Science and Technology Foundation. We thank S Nijsten and H Sun for assistance during parts of this work.

References

[1] Oehrlein G S and Williams H L 1987 *J. Appl. Phys.* **62** 662
[2] Oehrlein G S, Robey S W and Lindström J L 1988 *Appl. Phys. Lett.* **52** 1170
[3] Oehrlein G S 1993 *J. Vac. Sci. Technol.* A **11** 38
[4] Lowenstein L M 1988 *J. Vac. Sci. Technol.* A **6** 1984
[5] Nishino H, Hayasaka N, Horioka K, Shiozawa J, Nadahara S, Shooda N, Akema Y, Sakari A and Okano H 1993 *J. Appl. Phys.* **74** 1349
[6] Hattangady S V, Posthill J B, Fountain G G, Rudder R A, Mantini M J and Markunas R J 1991 *Appl. Phys. Lett.* **59** 339
[7] Beulens J J, Kastenmeier B E E, Matsuo P J and Oehrlein G S 1995 *Appl. Phys. Lett.* **66** 2634
[8] Bell F H, Joubert O, Oehrlein G S, Zhang Y and Vender D 1994 *J. Vac. Sci. Technol.* A **12** 3095
[9] Keller J H, Forster J C and Barnes M S 1993 *J. Vac. Sci. Technol.* A **11** 2487
[10] Mogab C J, Adams A C and Flamm D L 1978 *J. Appl. Phys.* **49** 3796
[11] D'Agostino R, Cramarossa F, De Benedictis S and Ferraro G 1981 *J. Appl. Phys.* **52** 1259
[12] Donnelly V M, Flamm D L, Dautremont-Smith W C and Werder D J 1984 *J. Appl. Phys.* **55** 242
[13] Kastenmeier B E E, Matsuo P J, Beulens J J and Oehrlein G S 1996 *J. Vac. Sci. Technol.* submitted for publication
[14] Matsuo P J, Kastenmeier B E E, Beulens J J and Oehrlein G S 1996 *J. Vac. Sci. Technol.* submitted for publication
[15] Ono K, Oomori T, Tuda M and Namba K 1992 *J. Vac. Sci. Technol.* A **10** 1071
[16] Cheng C C, Guinn K V, Donnelly V M and Herman I P 1994 *J. Vac. Sci. Technol.* A **12** 2630
[17] Herman I P, Donnelly V M, Guinn K P and Cheng C C 1994 *Phys. Rev. Lett.* **72** 2801
[18] Haverlag M, Vender D and Oehrlein G S 1992 *Appl. Phys. Lett.* **61** 2875
[19] Oehrlein G S, Zhang Y, Vender D and Haverlag M 1994 *J. Vac. Sci. Technol.* A **12** 323
[20] Oehrlein G S, Zhang Y, Vender D and Joubert O 1994 *J. Vac. Sci. Technol.* A **12** 333
[21] Winters H F and Coburn J W 1992 *Surf. Sci. Rep.* **14** 161
[22] Butterbaugh J W, Gray D C and Sawin H H 1991 *J. Vac. Sci. Technol.* B **9** 1461